Available online at www.sciencedirect.com
ScienceDirect
Catalysis Today 130 (2008) 32–40
CATALYSIS TODAY
www.elsevier.com/locate/cattod

Genesis of new gas oil HDS catalysts: Study of their liquid phase sulfidation

Naïma Frizi [a], Pascal Blanchard [a,*], Edmond Payen [a], Pascale Baranek [a], C. Lancelot [a], Michael Rebeilleau [b], Carole Dupuy [b], Jean Pierre Dath [b]

[a] *Unité de Catalyse et de Chimie du Solide, UMR CNRS 8181, Université des Sciences et Technologies, 59655 Villeneuve d'Ascq, France*
[b] *Total Petrochemicals Research, Zone industrielle CB-7181, Feluy, Belgique*

Abstract

The performance of gas oil hydrodesulfurization catalysts was successfully improved through the modification of oxidic precursors with thioglycolic acid. XPS study indicates that addition of this chelating agent affects the sulfidation of the supported metals. The higher catalytic performance was attributed to an optimization of the nature and morphology of the active phase due to the use of this chelating agent which enables a simultaneous sulfidation of both Co and Mo atoms.

Keywords: Hydrotreatment; MoS_2; Gas oil; Sulfidation; CoMo catalysts; HDS; Complexing agent; Morphology; Activation

1. Introduction

The new severe environmental regulations concerning the reduction of sulfur content in diesel oil impose a drastic improvement of the hydrodesulfurization (HDS) of petroleum feedstocks, which is a catalytic process most generally performed on $CoMo/Al_2O_3$ catalysts. The active catalysts are obtained by sulfiding an oxidic precursor, which is generally prepared by incipient wetness impregnation of an alumina support with an aqueous solution containing the elements to be deposited (Co and Mo), followed by a drying and a calcination step. It is now well accepted that the active phase is the so-called CoMoS phase. This phase consists of well-dispersed MoS_2 nanocrystallites decorated with Co promotor atoms, which are located at the edges and corners of the disulfide slabs [1]. The catalyst preparation is therefore a key step to reach high activities and to avoid any loss of cobalt atom in the alumina support thus forming $CoAl_2O_4$ type species [2], which are not easily sulfidable. These Co atoms are not available to promote the molybdenum disulfide slabs. Moreover during the sulfidation, inactive bulk Co_9S_8 entities may also be formed, which is also detrimental for the catalyst performance. Recently, new methods of preparation of the oxidic precursors have been developed in order to improve the catalytic performance of these solids. The addition of organic chelating agents in the impregnation solutions used for the preparation of these alumina supported CoMo-based oxidic precursors underwent a rapid development. Whatever the nature of the chelating agent and the thermal treatment, several hypotheses have been proposed to explain their exact role. However, in all cases, it was stated that they help to optimize the formation of the CoMoS phase through:

(i) an improvement of the Mo and/or Co dispersion [2–9] and a decrease in the Co fraction in the cobalt aluminate phase [2],
(ii) the modification of the relative rates of sulfidation of Co and Mo atoms [10–18],
(iii) a reduction of the interaction between the metals and the support [19–24].

A new approach for improving the performance of hydrotreating catalysts using various organic agents has been developed in our laboratory [25]. It consists of impregnating a conventional $CoMo/Al_2O_3$ oxidic precursor which has already been calcined with a solution containing the organic agent. In

* Corresponding author. Tel.: +33 0 320336017; fax: +33 0320436561.
E-mail address: pascal.blanchard@univ-lille1.fr (P. Blanchard).

0920-5861/$ – see front matter
doi:10.1016/j.cattod.2007.10.008

the present study, we first propose to use thioglycolic acid (TGA) aqueous solution, a chelating agent which can also be used as a sulfiding compound as was patented by the Sumitomo Metal Mining Company [26]. After the preparation of the so modified oxidic precursors, a detailed characterization of the genesis of the active phase is described. Then the catalytic performance of the modified catalyst in HDS of straight run gas oil is correlated to the nature and the morphology of the active phase as deduced from the study of the sulfidation, which enables us to understand the exact role of this chelating agent.

2. Experimental

2.1. Preparation of the oxidic precursors

The $CoMo/Al_2O_3$ catalyst used in this work is a calcined commercial catalyst containing 18 wt.% MoO_3 and 3.5 wt.% CoO. This oxidic precursor will be denoted hereafter CoMoRef.

For comparison purposes, a Mo/Al_2O_3 oxidic precursor was prepared by incipient wetness impregnation of commercial γ-Al_2O_3 extrudates (water pore volume: 1 $cm^3\ g^{-1}$; specific surface area: 350 $m^2\ g^{-1}$) with an ammonium heptamolybdate (AHM) aqueous solution, the AHM concentration being chosen to prepare a 20 MoO_3 wt.% solid. Similarly, a Co/Al_2O_3 oxidic precursor was prepared by impregnation of the γ-Al_2O_3 with an aqueous solution containing cobalt nitrate and ethylenediamine according to the method described by Blanchard et al. [2–4]. This method allows preparing a solid with a Co loading of 4 wt.% as CoO without formation of any bulk Co_3O_4. The impregnated extrudates were then dried at 100 °C overnight and calcined in air at 500 °C for 4 h. The Mo/Al_2O_3 and the Co/Al_2O_3 oxidic precursors are denoted MoRef and CoRef, respectively.

2.2. Preparation of the modified oxidic precursors

The CoMoRef, CoRef and MoRef calcined oxidic precursors were pore volume impregnated with an aqueous solution containing the desired amount of thioglycolic acid. After 2 h of aging, the so obtained modified solids were dried at 80 °C under N_2 during 15 h but were not calcined. Several TGA/Mo molar ratios were studied and these modified catalysts are denoted as MoXTGA and CoMoXTGA, where X is the TGA/Mo molar ratio. In the case of the Co/Al_2O_3-based solid, the modified solids are denoted CoXTGA but for comparison purposes the amounts of TGA impregnated correspond to those added for CoMoXTGA.

2.3. Catalytic activities

The catalysts were tested in a high pressure up-flow microreactor to evaluate the catalytic behavior with real feedstock. The microreactor unit had a cylindrical reactor with an inside diameter of 0.8 cm and a length of 72 cm. The temperature in the reactor was measured and regulated at different levels using 10 thermocouples enabling us to have an isothermal zone in the middle of the reactor (40 cm). The feed was pumped from a stainless steel tank to the reactor using a HPLC pump. The desired pressure of reaction was controlled by pressure regulators and controllers. For each test 10 mL of catalyst extrudates (4 mm length) diluted with 15 mL of carborundum (0.25 mm) were loaded in the isothermal zone of the reactor. Carborundum (0.5 and 1.19 mm) was placed above and below the catalyst bed.

Prior to the sulfidation, the catalysts were dried at atmospheric pressure under a nitrogen flow at 300 °C for 3 h (temperature rate = 60 °C h^{-1}) for the CoMoRef oxidic precursor and at 80 °C during 60 h (temperature rate = 60 °C h^{-1}) for the modified catalysts.

The catalysts were sulfided using a mixture of dimethyldisulfide (DMDS), straight run gas oil (SRGO) (2 wt.% DMDS + SRGO) and H_2. The characteristic of the SRGO are presented in Table 1. The catalysts were soaked with this sulfiding feed in hydrogen atmosphere (35 bars) at 80 °C, using a liquid hourly space velocity (LHSV) of 6 h^{-1}. Then the LHSV was decreased to 2 h^{-1} (with H_2/oil = 250 NL/L) and the bed temperature was raised to 110 °C at a rate of 30 °C h^{-1} and stabilized for 3 h at the same temperature. The catalyst bed temperature was further increased to 220 °C at a rate of 30 °C h^{-1} and stabilized for 3 h. The final temperature of sulfidation was 350 °C (ramping rate of 30 °C h^{-1}) and it was stabilized for 11 h.

After sulfidation, the feed was switched to the test feed (same SRGO as for sulfidation), the operating conditions being as follows: pressure = 35 bars; H_2/oil = 250 NL/L; LHSV = 2 h^{-1}. During each run, the temperature was changed in the sequence 350–360–370 °C. Two hydrotreated product samples were collected at each temperature after stabilization for 15 h. H_2S dissolved in the hydrotreated product oil was removed by stripping with nitrogen gas after sample collection.

The total sulfur contents of feed and product samples were determined using an Antek 9000S sulfur analyzer (Ultra-Violet fluorescence). Individual sulfur compound distributions in different samples were determined using a VARIAN CP-3800 gas chromatograph system with autosampler/injector equipped with a 25 m × 0.32 mm × 0.12 μm CP-SIL 5 CB capillary column (Chrompack) and a Sulfur Chemiluminescence Detector-SCD (Sievers model 355).

2.4. Characterization techniques

2.4.1. XPS

The catalysts were characterized by X-ray photoelectron spectroscopy (XPS) at different stages of the activation. The catalysts were sulfided using the same procedure as described above. When the desired temperature was reached, the reactor was cooled down very quickly under hydrogen and gas oil flow. After depressurizing the reactor, the catalyst was dried at

Table 1
Main characteristic of the SRGO

Sulfur concentration (wppm)	9939
Total aromatics (wt.%)	24.3
Total nitrogen concentration (wppm)	171
Density at 15 °C (g/mL)	0.842

ambient temperature under nitrogen flow in the reactor to remove the residual gas oil and transferred under nitrogen flow in a container filled with toluene. After filtration, the solid was washed with pentane and dried under nitrogen at 45 °C for 15 h to remove this solvent. The preparation of XPS specimen was performed under argon atmosphere in a glove box in order to avoid any reoxidation of the solids.

The powdered samples were pressed into an indium foil attached to the sample holder, which was introduced directly in the XPS spectrometer, via the connection of the glove box to the XPS transfer chamber of the spectrometer. XPS spectra were recorded with the VG ESCALAB 220 XL spectrometer equipped with a monochromatic Al Kα (E = 1486.6 eV) X-ray source. The spectra were collected with a pass energy of 30 eV, using the electromagnetic lens mode low-energy electron flood gun for charge compensation effect. The binding energies (BE) of Mo3d, Co2p, C1s and S2p were determined by computer fitting of the measured spectra and referred to the Al2p photopeak of the support at 74.6 eV. The binding energies were estimated to within ±0.2 eV. The surface atomic ratios I_{Mo3d}/I_{Al2p} and I_{Co2p}/I_{Al2p} were calculated using the VG Eclipse software after subtracting the nonlinear Shirley background and the contribution of the S2s signal to the Mo3d one. The Mo3d and Co2p spectra were decomposed using an interactive least-squares program and the fitting peaks of the experimental curves were defined using a combination of Gaussian (70%) and Lorentzian (30%) distributions. The decompositions were performed to quantify the fraction of Mo and Co, which have been chelated by TGA after modification of the oxidic precursor by TGA and to estimate the percentages of Mo atoms, which form the MoS_2 slabs, and of Co atoms involved in the sulfidic phase (i.e. CoMoS + Co_9S_8) after sulfidation. These percentages will be hereafter noted ''Mo sulfidation degree'' and ''Co sulfidation degree''. The surface quantification is based on the peak surface areas relative to each chemical species present on the surface of the solid. The methodology implemented for the decomposition of the oxidic precursors spectra as well as of the modified ones before and after sulfidation has been described elsewhere [27]. The S2s peak, which contributes to the total envelope of the spectra of Mo3d, was simulated with only one peak by taking as reference the S2p peak with respect to the following criteria: BE(S2s)−BE(S2p) = 64 eV. The contribution of the oxidic state to the Mo3d spectrum was determined from the analysis of the reference oxidic precursor. This contribution was introduced in the spectra of the modified solids. Other contributions were then introduced in order to fit the overall spectrum. For the sulfided catalysts, the Mo3d spectra were decomposed similarly into the three well-known contributions respectively attributed to Mo^{VI}oxide ($Mo3d_{5/2}$ BE = 233,0 eV), Mo^{V}oxysulfide ($Mo3d_{5/2}$ BE = 230.5 eV) and Mo^{IV} (MoS_2) ($Mo3d_{5/2}$ BE = 228.8 eV) [28]. For Co2p core level, the methodology consisted in isolating successively the contributions of each Co-based chemicals species and to decompose the spectra by varying only the global intensity of each contribution to obtain the relative amount of each species. Each contribution was simulated with four peaks corresponding to the $Co2p_{3/2}$ (main peak + satellite structure) and $Co2p_{1/2}$ (main peak + satellite structure) core levels. For each contribution, the spectral parameters [i.e. the BE differences, the intensity ratios and the Full Width at Half Maximum (FWHM) ratios] of these four peaks are interdependent whatever the decomposition. Two contributions were used for the modified oxidic precursors considering onlys the presence of two states for the Co atoms, i.e. Co^{2+} in oxidic state and Co^{2+} chelated by TGA, while for sulfided catalysts Co^{2+} in oxidic state and Co^{2+} in sulfur environment (peaks respectively at 781.8 and 778.7 eV) were considered.

The absence of any signal at 169.0 eV (characteristic of sulfates) indicates that no reoxidation of the sulfided catalysts occurred during the transfer of the solid from the sulfiding reactor to the XPS machine.

2.4.2. Raman spectroscopy

The Raman spectra of the samples maintained at room temperature were recorded using a Raman microprobe (Infinity from Jobin-Yvon) equipped with a photodiode array detector. The exciting laser source was the 532 nm line of a Nd-YAG laser with a beam power of 0.23 mW at the focal point. The wavenumber accuracy was 2 cm^{-1}.

2.4.3. High resolution electron microscopy (HREM)

High resolution electron microscopy was performed on a TECNAI TEM (200 kV) equipped with a LaB_6 filament. Freshly sulfided samples were ground under an inert atmosphere and dispersed in heptane. The suspension was collected on a microscope grid covered with a thin lacey carbon film. For statistical analysis, more than 20 photographs were taken, which enabled us to measure about 2000 slabs for each sample. Statistical analysis of each photograph was done by measuring the length (L) and stacking (N) of the MoS_2 slabs.

3. Results

3.1. Reactivity

Fig. 1 shows the catalytic performance of the CoMoRef and CoMoXTGA catalysts (X is the TGA/Mo molar ratio, X = 1, 2

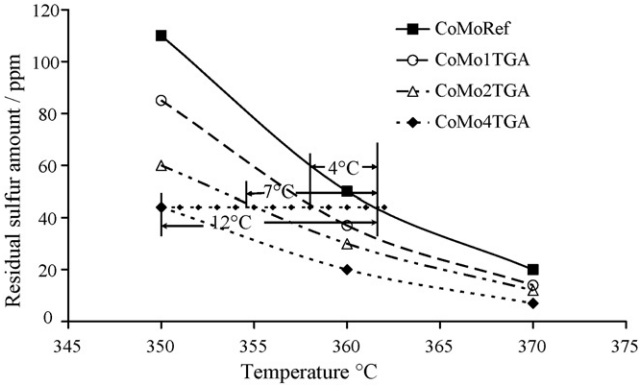

Fig. 1. Catalytic performance of the CoMoRef and CoMoXTGA solids (X is the TGA/Mo molar ratio) in HDS of a Straight Run Gas Oil: Residual sulfur content in the desulfurized feed versus the temperature of the reactor.

and 4). For each catalyst, the residual sulfur content in the hydrotreated product is plotted as a function of the reactor temperature. This shows that the modification of the conventional solid by TGA induces an increase in the catalytic performance and enables to obtain very low residual sulfur content at lower temperature than that required by the oxidic precursor. Moreover, it shows that the improvement depends on the amount of chelating agent added, the best improvement being obtained with a TGA/Mo ratio of 4. Physico-chemical characterization of the CoMoRef and CoMo4TGA catalysts was performed at each step of the genesis of the active phase in order to understand the exact role of this chelating agent.

3.2. Characterization of modified oxidic precursors

In a previous study, we showed by Raman spectroscopy that Mo was well dispersed on the alumina surface. Indeed, the spectra of MoRef (Fig. 2b) and CoMoRef (Fig. 2c) catalysts do not exhibit any features of bulk oxides such as MoO_3 or $CoMoO_4$, while they exhibit a main line at 950 cm^{-1} which is characteristic of the presence of well-dispersed polymolybdate species [29]. Moreover, Diffuse Reflectance UV-Visible spectroscopy confirms the absence of bulk Co_3O_4. It has also been shown by Raman spectroscopy that, upon modification by TGA, both elements Co and Mo were chelated by the TGA [27]. Typical Raman spectra of the TGA modified oxidic precursors are given in Fig. 2. The spectra of Co4TGA (Fig. 2d) and CoMo4TGA (Fig. 2f) exhibit Raman lines at 260 and 377 cm^{-1}, respectively, assigned to Co–S and Co–O vibrations in Co–TGA complexes [30]. The spectra of Mo4TGA (Fig. 2e) and CoMo4TGA (Fig. 2f) present lines at 396 and 960 cm^{-1}, which are respectively assigned to Mo–S and Mo–O vibrations in Mo–TGA complexes [31–34]. However, the main line characteristic of the starting oxomolybdate phase was always observed, suggesting that the chelation of the Mo atoms is not complete. It has also been shown that all the TGA molecules are coordinated through the sulfur atom and the carboxyl group. The modification of the CoMo oxidic precursor upon addition of TGA was also clearly shown by XPS. The Mo3d spectrum of the reference oxidic precursor (Fig. 3.A.a) exhibits a $Mo3d_{5/2}$ photopeak with an apparent binding energy (BE) of 233.0 eV, which is characteristic of Mo^{VI} in oxidic environment. Introduction of TGA results in a shift and broadening of the Mo3d spectrum shape (Fig. 4.A.a) which was assigned to the formation of Mo^{V}–TGA complexes [35]. The decomposition of the Mo3d spectrum of the modified solid allowed estimating that 75% of the Mo atoms were chelated by TGA, in agreement with the Raman analysis. Figures 3.B.a and 4.B.a respectively show the Co2p XPS spectra of the CoMoRef and CoMo4TGA samples. The complexation of the Co upon TGA addition was indicated by a shift of the Co2p peaks, while the Co2p spectrum decomposition of the CoMo4TGA solid enabled us to estimate that 50% of the Co atoms were chelated by TGA.

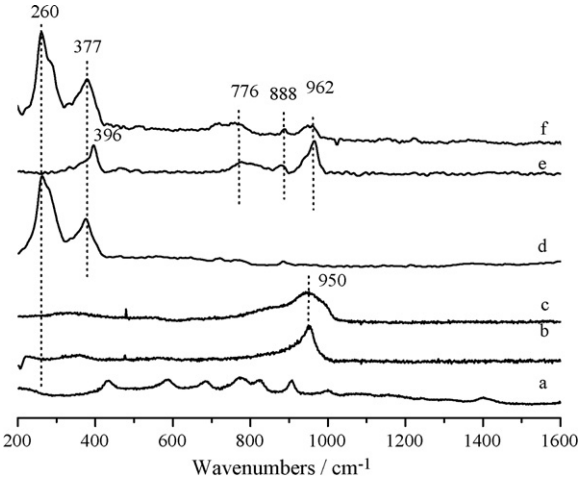

Fig. 2. Raman spectra in the 200–1600 cm^{-1} spectral range of: (a) TGA aqueous solution, (b) MoRef, (c) CoMoRef, (d) Co4TGA, (e) Mo4TGA and (f) CoMo4TGA.

3.3. Characterization of the sulfided catalysts

3.3.1. XPS characterizations

Figures 3.A.e, 3.B.e, 4.A.e and 4.B.e show the XPS spectra of the CoMoRef and CoMo4TGA after sulfidation at 350 °C for 11 h. Whatever the solid, the Mo spectra exhibit a $Mo3d_{5/2}$ photopeak at 228.8 eV characteristic of MoS_2, while there is a

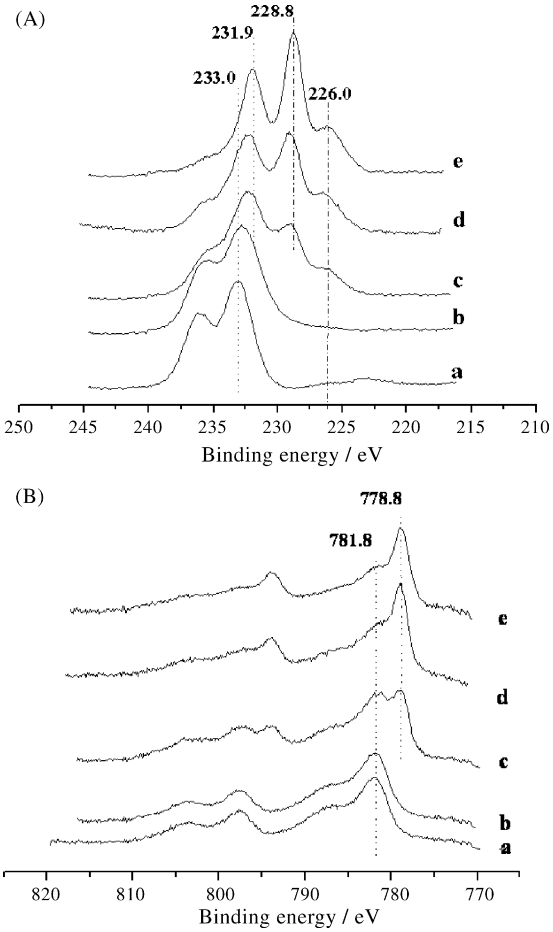

Fig. 3. XPS spectra of CoMoRef at different stages of the liquid phase sulfidation. (A) Mo3d spectra: (a) unsulfided, (b) 110 °C 3 h, (c) 220 °C 3 h, (d) 280 °C and (e) 350 °C 11 h. (B) Co2p spectra: (a) unsulfided, (b) 110 °C 3 h, (c) 220 °C 3 h, (d) 280 °C and (e) 350 °C 11 h.

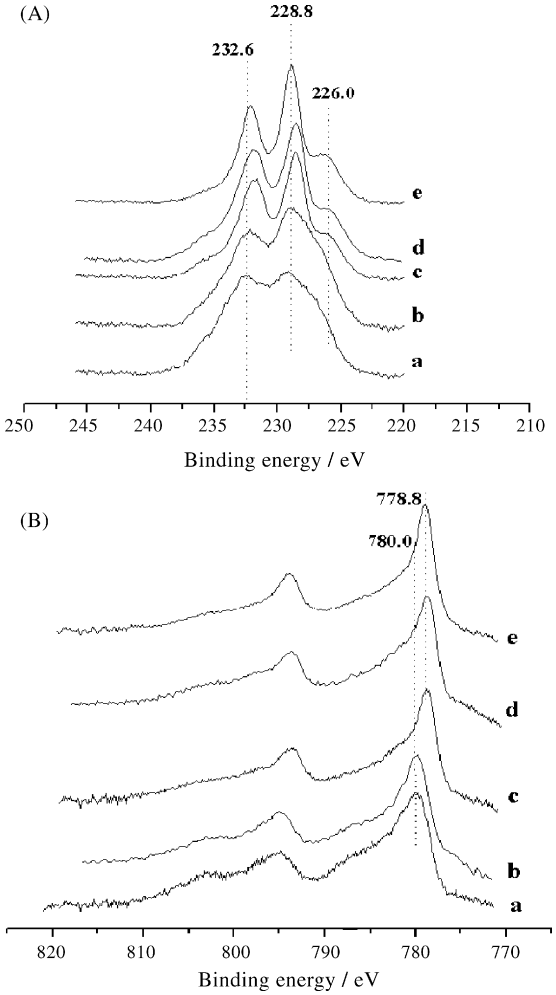

Fig. 4. XPS spectra of CoMo4TGA at different stages of the liquid phase sulfidation. (A) Mo3d spectra: (a) unsulfided, (b) 110 °C 3 h, (c) 220 °C 3 h, (d) 280 °C and (e) 350 °C 11 h. (B) Co2p spectra: (a) unsulfided, (b) 110 °C 3 h, (c) 220 °C 3 h, (d) 280 °C and (e) 350 °C 11 h.

$Co2p_{3/2}$ peak at about 778.7 eV in the Co spectra characteristic of Co in a sulfur environment. The I_{Mo3d}/I_{Al2p} and I_{Co2p}/I_{Al2p} ratios reported in Table 2 show that the dispersion of the molybdenum is not affected by the TGA modification and sulfiding treatment, whereas a slight increase in the I_{Co2p}/I_{Al2p} ratio is observed, which may suggest a redispersion of cobalto species. Whatever the catalyst, according to Topsøe et al. [36], the binding energy differences $BE(Co2p_{3/2})-BE(S2p)$ and $BE(Co2p_{3/2})-BE(Mo3d_{5/2})$ given in Table 3 are characteristic for cobalt atoms decorating the MoS_2 phase. Nevertheless, the shape of the XPS spectra of Co2p and Mo3d core level after

Table 2
Dispersion of Mo and Co for the CoMoRef and CoMo4TGA solids before and after sulfidation at 350 °C under liquid phase (SRGO + DMDS) as determined by XPS

Samples	I_{Mo3d}/I_{Al2p}	I_{Co2p}/I_{Al2p}
CoMoRef	1.50	0.89
CoMo4TGA	1.37	1.02
Sulfided CoMoRef	1.49	1.01
Sulfided CoMo4TGA	1.51	1.21

Table 3
XPS data of the CoMoRef and CoMo4TGA catalysts sulfided under liquid phase (SRGO + DMDS) at 350 °C

Catalysts	CoMoRef	CoMo4TGA
$BE(Co2p_{3/2})-BE(Mo3d_{5/2})$ (eV)	550	550
$BE(Co2p_{3/2})-BE(S2p)$ (eV)	616.8	616.8
Co sulfidation degree (%)	52	60
Mo sulfidation degree (%)	69	76

sulfidation at 350 °C of CoMo4TGA is better resolved, indicating that TGA induces a better sulfidation of molybdenum and cobalt atoms. A decomposition of the XPS Mo3d and Co2p peaks (Figs. 5.a and 5.b, respectively) was performed for both catalysts with the aim to determine the Mo and Co sulfidation degrees, which are reported in Table 3. They confirm that the modification of the reference catalyst by TGA induces an increase in both Co and Mo sulfidation degrees.

3.3.2. TEM

The sulfided catalysts were analyzed using TEM to determine the effect of the addition of TGA on the MoS_2 morphology. Typical TEM images are given in Fig. 6, whereas the distribution

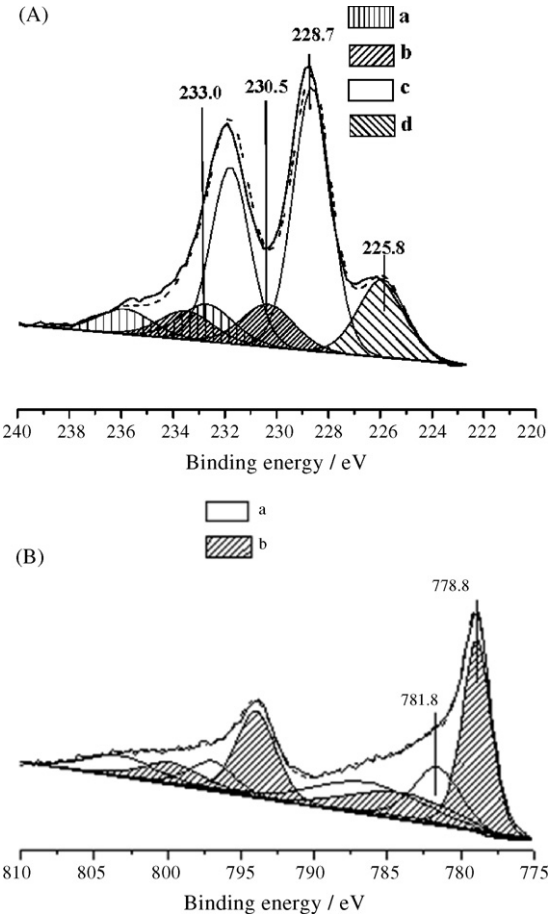

Fig. 5. Examples of decompositions of XPS spectra after sulfidation at 350 °C. (A) Mo3d spectrum: (a) contribution of Mo^{VI} oxidic phase, (b) contribution of Mo^{V} oxysulfide phase, (c) contribution of $Mo^{IV}S_2$ phase and (d) contribution of S2s. (B) Co2p spectrum: (a) contribution of Co^{II} oxidic phase and (b) contribution of Co atoms in sulfidic phases.

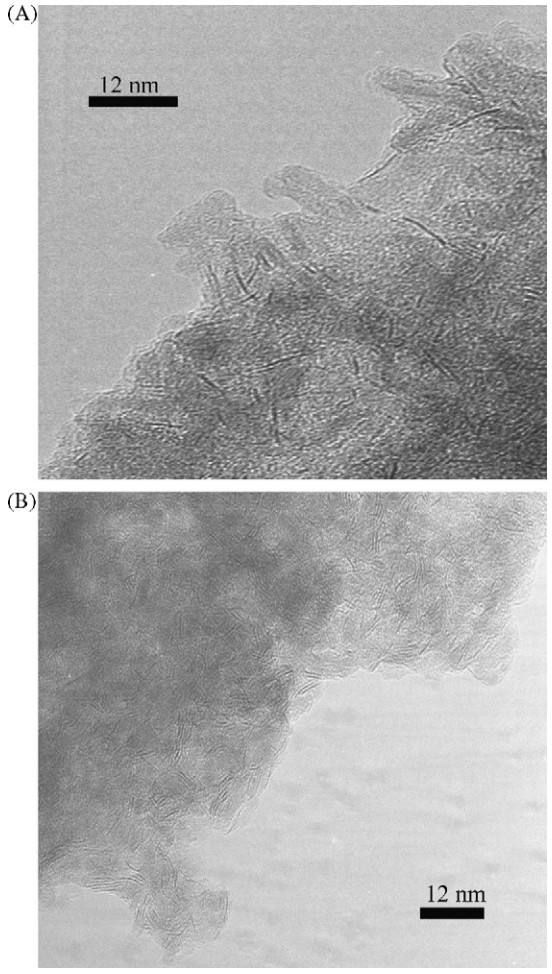

Fig. 6. Typical HREM micrographs of (a) sulfided CoMoRef and (b) sulfided CoMo4TGA.

of the lengths and stacking degree of MoS_2 slabs are reported in Fig. 7. For the CoMoRef catalyst, the slab length distribution is centered on the [2.6–3.9 nm] interval. 28% of the detected slabs have a length lower than 2.6 nm and 36% of the slabs have a length higher than 3.9 nm. Moreover, single-layered slabs are predominant (57% of the detected slabs), only 6% presenting a stacking higher than two layers. These results are in agreement with literature data, which show that liquid phase sulfidation mainly gives single slabs [37]. On the TGA modified catalyst, these distributions are very different. Indeed, 37% of the detected slabs have a length lower than 2.6 nm. It is also shown that only 29% of the slabs have a length higher than 3.9 nm. Moreover, whereas the CoMoRef presents mostly single slabs, the CoMo4TGA contains a larger amount of two-layered slabs and 16.5% of the detected slabs present a stacking equal or higher than three layers. So, TEM shows that the modification of the oxide precursor by TGA has a strong influence on the morphology of the active phase, inducing an increase in the stacking as well as a decrease in the MoS_2 slabs length.

3.4. Characterization of the catalysts during the sulfidation

It thus appears that the TGA induces a modification of the morphology of the active phase which is not directly explained by the nature of the supported oxide phases. A detailed study of the sulfidation was therefore undertaken.

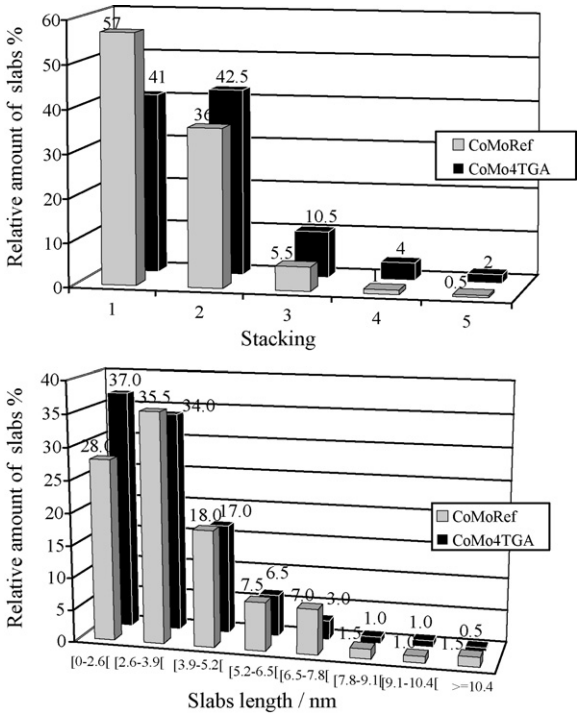

Fig. 7. Distribution of the length and stacking of the MoS_2 slabs of the CoMoRef and CoMo4TGA catalysts after sulfidation under liquid phase at 350 °C for 11 h.

3.4.1. XPS study of C1s and S2p core levels

The relative amounts of sulfur introduced in the CoMoRef and CoMo4TGA catalysts were evaluated during the sulfidation by measuring the corresponding $I(S_{2p})/I(Al_{2p})$ intensity ratios at different stages of the sulfidation treatment. The evolution of the $I(S_{2p})/I(Al_{2p})$ intensity ratio is reported in Fig. 8. This figure also presents the evolution of the C1s core level XPS peak at 289 eV, which is characteristic of the TGA carboxyl group in the metal–TGA entities, during the CoMo4TGA sulfidation. The relative concentration of this element is thus evaluated by the $I(C_{1sCOO})/I(Al_{2p})$ intensity ratio.

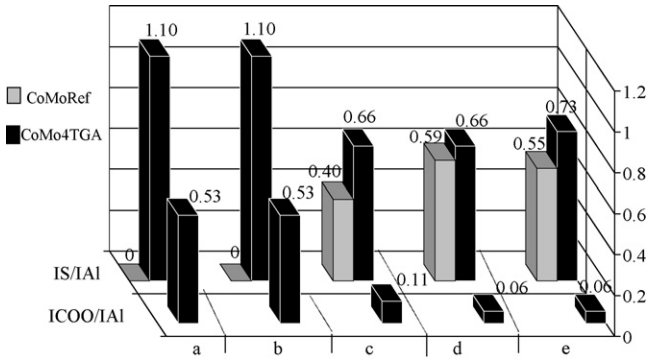

Fig. 8. $I(S_{2p})/I(Al_{2p})$ and $I(C_{1sCOO})/I(Al_{2p})$ XPS ratios (respectively, denoted as IS/IAl and ICOO/IAl) obtained at different stages of the liquid phase activation for the CoMoRef and CoMo4TGA catalysts: (a) unsulfided, (b) 110 °C 3 h, (c) 220 °C 3 h, (d) 280 °C and (e) 350 °C 11 h.

The evolution of the $I(S_{2p})/I(Al_{2p})$ ratio is very different for both solids. For the CoMoRef catalyst, the $I(S_{2p})/I(Al_{2p})$ ratio only increases after sulfidation at 220 °C for 3 h indicating that sulfur is introduced in the solid between 110 °C and the end of the treatment at 220 °C. This is in agreement with the production of H_2S in the reactor. Indeed, Texier et al. indicate that the decomposition of DMDS into H_2S and CH_4 starts at about 160 °C [38].

In the case of the CoMo4TGA, the $I(S_{2p})/I(Al_{2p})$ and the $I(C_{1sCOO})/I(Al_{2p})$ ratios remain constant after sulfidation at 110 °C for 3 h, whereas a drastic decrease is observed after sulfidation at 220 °C for 3 h. This means that the TGA-based species are mainly decomposed at the end of this latter stage, in agreement with a previous study [27], in which we have shown that the Mo–TGA and Co–TGA complexes are stable up to 220 °C under H_2/H_2S atmosphere. After activation at 350 °C for 11 h, the $I(S_{2p})/I(Al_{2p})$ ratio obtained for the CoMo4TGA is higher than that of the CoMoRef, in agreement with the Mo and Co sulfidation degrees given in Table 3.

3.4.2. XPS study of Co2p and Mo3d core levels

3.4.2.1. Evolution of the CoMoRef during the sulfidation. Figures 3.A and 3.B respectively show the evolution of the Mo3d and Co2p XPS spectra of the CoMoRef at the different stages of the sulfidation. The BE of the Mo3d does not change after activation at 110 °C for 3 h and no sulfidic components are observed (Fig. 3.A.b). This shows that no sulfidation of the Mo atoms occurs at this temperature, as suggested in Fig. 8. However, a small peak broadening is observed, which suggests that a reduction of a small amount of Mo atoms into Mo^V oxospecies occurs since no H_2S is present in the reactor at this temperature. After activation at 220 °C for 3 h (Fig. 3.A.c), a contribution of Mo in sulfidic state (BE = 228.8 eV) is observed, in agreement with the above mentioned evolution of the $I(S_{2p})/I(Al_{2p})$ ratio (Fig. 8). This suggests that molybdenum sulfidation starts at a temperature between 110 and 220 °C, most probably at 160 °C, i.e. temperature at which the DMDS starts to decompose into CH_4 and H_2S [38]. Then, the spectrum of molybdenum evolves continuously from 220 °C up to 350 °C (Fig. 3A.c–e). Indeed, the Mo XPS features of the oxidic components (BE = 233 eV) gradually disappear, while those of the sulfidic components increase (BE = 228.8 eV) with increasing the sulfidation temperature up to 350 °C. At low temperatures, the evolution of the Co2p spectrum is similar to that of Mo. Indeed, after activation at 110 °C, no sulfidation of Co is observed (Fig. 3.B.b), whereas after activation at 220 °C for 3 h, a contribution of Co in sulfidic state (BE = 778.8 eV) is observed (Fig. 3.B.c). This suggests that the sulfidation of Co starts also at a temperature between 110 and 220 °C. Nevertheless, the Co2p spectra obtained after activation at 280 °C and after activation at 350 °C for 11 h are quite similar (Fig. 3.B.d, e), their full width at half maximum being exactly the same (i.e. FWHM = 4.3 eV). This shows that the sulfidation of Co is already complete at 280 °C. So, taking into account the decomposition of DMDS into H_2S and CH_4 which starts at 160 °C, we can propose that the sulfidation of Co and Mo starts at 160 °C, in agreement with the XPS results. Nevertheless, the sulfidation of Co ends before that of Mo.

3.4.2.2. Evolution of the CoMo4TGA during the sulfidation. Figures 4.A and 4.B respectively show the evolution of the Mo3d and Co2p XPS spectra of the CoMo4TGA at the different stages of the sulfidation. The Co2p and Mo3d spectra do not change after activation at 110 °C for 3 h. The shape of the Mo3d is only slightly affected (Fig. 4.A.b), which suggests a small reduction of the Mo atoms as confirmed by the constant $I(S_{2p})/I(Al_{2p})$ and $I(C_{1sCOO})/I(Al_{2p})$ ratios. After sulfidation at 220 °C for 3 h, the $Co2p_{3/2}$ peak (Fig. 4.B.c) shifts toward lower BE, while the shape of the Mo3d spectrum (Fig. 4.A.c) clearly shows the formation of MoS_2. Moreover, the $I(S_{2p})/I(Al_{2p})$ and $I(C_{1sCOO})/I(Al_{2p})$ ratios drastically decrease (Fig. 8). This confirms that the Co–TGA and Mo–TGA complexes are mainly decomposed during this stage of the activation, inducing the sulfidation of the metals. Upon increasing the temperature, the Mo3d and Co2p spectra evolve continuously up to the end of activation at 350 °C. In particular, the FWHM of the $Co2p_{3/2}$ peak (Fig. 4.B.d, e) decreases from 3.4 to 2.9 eV between 280 and 350 °C, which shows that the sulfidation of Co is complete only after treatment at 350 °C for 11 h. In the same way, the evolution of the Mo3d spectrum (Fig. 4.A.d, e) highlights that its sulfidation is completed after activation at 350 °C for 11 h.

Thus, this study shows that the modification with TGA induces differences in the evolution of the metals during the liquid phase activation. Indeed, the sulfidation of Co is completed before that of Mo in the CoMoRef, while the sulfidation of both Mo–TGA and Co–TGA species occurs simultaneously in the same range of temperatures, i.e. from 220 to 350 °C.

4. Discussion

It has thus been shown that impregnating a classical CoMo-based oxidic precursor with TGA aqueous solution induces an improvement of the gas oil HDS performance. As the active phase is still the CoMoS phase, this improvement of the catalytic performance should be explained by the modification of the exact nature of the CoMoS phase induced by the use of TGA.

XPS results show that the dispersion of the molybdenum is not affected by the modification with TGA. Thus, contrarily to previous studies where the aim was to improve the dispersion by the introduction of chelating agents in the impregnation solution [2–9], the objective here was to change the nature of the supported species, which will be sulfided. Indeed, whatever the complexing agent used in the aforementioned studies, a calcination step was performed before the sulfidation. Consequently, this was always the same type of oxomolybdate species, which were sulfided, the calcination being a levelling step for these modifications [2].

The modification of CoMoRef by TGA leads to an enhancement of the molybdenum sulfidation degree, whereas a decrease in the length of the MoS_2 slabs is indicated by HREM. Both results suggest that a higher number of MoS_2

slabs and accordingly a higher number of active sites are generated on the modified catalysts. This effect could be assigned to the modification of the nature of the supported species, which are sulfided during the activation. The same effect is observed for the cobalt atoms. Indeed, the TGA induces a higher cobalt sulfidation degree, which should also be considered to explain the improvement of the performance. In agreement with the evolution of the I_{Co2p}/I_{Al2p} ratio, it can be suggested that some Co^{2+} atoms of the aforementioned $CoAl_2O_4$ surface species, which are not supposed to be easily sulfidable, are used for the promotion because of the presence of the chelating agent.

Moreover, we have shown that, under activation in liquid phase, the sulfidation of both Mo and Co starts at 160 °C for the reference oxidic precursor, the sulfidation of Co being complete before that of Mo. The modification with TGA induces a beginning of the sulfidation of both metals at 220 °C due to the stability of Mo–TGA and Co–TGA species toward the sulfidation, leading to a simultaneous sulfidation of both Mo and Co atoms. We may suggest that this inhibits the formation of Co_9S_8, making more Co atoms available for the decoration position. Several authors proposed that the improvement of the HDS performance obtained through the use of complexing agents (En, EDTA, CyDTA or NTA...) in the impregnation solution used for the preparation of oxidic precursors could be assigned to the modification of the genesis of the active (Ni)CoMoS phase if the catalysts are not calcined before the sulfidation [10–18]. They suggested that the Co ions would be able to disperse themselves over the edges of the MoS_2 crystallites if the sulfidation of Co was proceeding after the formation of the MoS_2 slabs. In contrast to that, without any complexing agent, the sulfidation of Co would be complete before the formation of MoS_2 slabs, yielding bulk Co_9S_8 formation, the Co atoms of which would not be available to promote the MoS_2 slabs at higher temperatures [39]. This was also observed in this work for the CoMoRef catalyst.

However, the simultaneous sulfidation of Co and Mo atoms can also be related to the decrease in the MoS_2 slabs size, which is observed for the CoMo4TGA. Indeed, the Co atoms would migrate on the MoS_2 edges during the formation of the MoS_2 slabs, which should block the growth of the MoS_2 in the lateral direction. This is in agreement with DFT calculations showing that sulfur atoms have a lower affinity to cobalt than to molybdenum [40]. So the presence of cobalt atoms in decoration position on the MoS_2 crystallite edges would prevent the growth of the slab. In contrast to that, if the sulfidation of Co is inhibited by a too strong chelating agent, whereas molybdenum sulfidation takes place, the MoS_2 slabs will consequently become longer. This is in agreement with the results recently obtained by Gonzalez-Cortés et al. [41], which show that an increase in the MoS_2 size is observed upon gas phase sulfidation of a $CoMo/Al_2O_3$ oxidic precursor prepared with such an amount of EDTA that only the Co atoms are chelated.

Finally, the higher stacking of the MoS_2 slabs induced by the use of TGA could also be considered to explain the improved performance in HDS of gas oil that we obtained. Indeed, it could correspond to the formation of the more active type II CoMoS phase, which was associated with stacked MoS_2 slabs [22]. Moreover, some authors proposed that stacked CoMoS phase should be more efficient for the desulfurization of large molecules such as dialkyl dibenzothiophenes [21,42], which are present in large amount in the real feed used in this work (Sievers-chromatogram not reported here). These hypotheses are nevertheless still controversial in the literature. Indeed, a recent work of Eijsbouts et al. showed that the most active commercially available Type 2 catalysts for ultra low sulfur desulfurization do not contain high amount of stacked MoS_2 slabs after liquid phase sulfidation [37]. They concluded that MoS_2 stacking is not required for the formation of the CoMoS II phase as well as for the desulfurization of molecules like 4,6-dialkyl dibenzothiophenes. Hensen et al. already observed the formation of such stacked slabs for Mo–NTA/Al_2O_3 systems and they attributed the stacking to a decrease in the Mo–alumina interaction due to the complexation of the metal by the NTA [42]. However, their results also show an increase in the length of the slabs. In the present work, both the decrease in the length of MoS_2 slabs and the increase in the stacking are obtained due to the use of the TGA modifying agent which enables to control the sulfidation of both metal atoms.

5. Conclusion

This work confirms that the liquid phase sulfidation of a conventional HDS CoMo catalyst is not optimized as the sulfidation of Co is completed before all the Mo atoms are transformed into MoS_2. This study clearly shows that the catalytic performance in HDS of gas oil of such a conventional oxidic precursor can be improved through its modification by the impregnation of a well-chosen chelating agent such as thioglycolic acid. It has been shown that the impregnation of thioglycolic acid induces a complexation of both metals, which leads to an optimization of the active phase through a better control of the Co and Mo sulfidation.

References

[1] H. Topsøe, B.S. Clausen, F.E. Massoth, Hydrotreating Catalysis, Springer, Berlin, 1996.
[2] P. Blanchard, C. Lamonier, A. Griboval, E. Payen, Appl. Catal. A: Gen. 322 (2007) 33.
[3] P. Blanchard, C. Mauchaussee, E. Payen, J. Grimblot, O. Poulet, N. Boisdron, R. Loutaty, Stud. Surf. Sci. Catal. 91 (1995) 1037.
[4] P. Blanchard, E. Payen, J. Grimblot, O. Poulet, R. Loutaty, Stud. Surf. Sci. Catal. 111 (1997) 211.
[5] Y. Yoshimura, T. Sato, H. Shimada, N. Matsubayashi, M. Imamura, A. Nishijima, M. Higo, S. Yoshitomi, Catal. Today 29 (1996) 221.
[6] Y. Yoshimura, N. Matsubayashi, T. Sato, H. Shimada, A. Nishijima, Appl. Catal. A: Gen. 79 (1991) 145.
[7] K. Inamura, K. Uchikawa, S. Matsuda, Y. Akai, Appl. Surf. Sci. 121/122 (1997) 468.
[8] R. Iwamoto, N. Kagami, A. Iino, J. Jap. Petrol. Inst. 48 (4) (2005) 237.
[9] R. Iwamoto, N. Kagami, Y. Sakoda, A. Iino, J. Jap. Petrol. Inst. 48 (6) (2005) 351.
[10] G. Kishan, L. Coulier, V.H.J. de Beer, J.A.R. van Veen, J.W. Niemantsverdriet, J. Catal. 196 (2000) 180.

[11] L. Coulier, G. Kishan, J.A.R. van Veen, J.W. Niemantsverdriet, J. Vac. Sci. Technol. A 19 (4) (2001) 1015.
[12] L. Coulier, V.H.J. de Beer, J.A.R. van Veen, J.W. Niemantsverdriet, J. Catal. 197 (2001) 26.
[13] G. Kishan, J.A.R. van Veen, J.W. Niemantsverdriet, Top. Catal. 29 (2004) 103.
[14] G. Kishan, L. Coulier, V.H.J. de Beer, J.A.R. van Veen, J.W. Niemantsverdriet, J. Chem. Soc. Chem. Commun. (2000) 1103.
[15] R. Cattaneo, Th. Weber, T. Shido, R. Prins, J. Catal. 191 (2000) 225.
[16] S.P.A. Louwers, R. Prins, J. Catal. 133 (1992) 94.
[17] G. Kishan, L. Coulier, J.A.R. van Veen, J.W. Niemantsverdriet, J. Catal. 200 (2001) 194.
[18] L. Coulier, G. Kishan, J.A.R. van Veen, J.W. Niemantsverdriet, J. Phys. Chem. B 106 (2002) 5897.
[19] R. Cattaneo, T. Shido, R. Prins, J. Catal. 185 (1999) 199.
[20] R. Cattaneo, F. Rota, R. Prins, J. Catal. 199 (2001) 318.
[21] M. Sun, D. Nicosa, R. Prins, Catal. Today 86 (2003) 173.
[22] J.A.R. van Veen, E. Gerkema, A.M. van der Kraan, A. Knoester, J. Chem. Soc. Chem. Commun. (1987) 1684.
[23] D. Nicosa, R. Prins, J. Catal. 229 (2005) 424.
[24] D. Nicosa, R. Prins, J. Catal. 234 (2005) 414.
[25] N. Frizi, Thesis, Lille, France (2004).
[26] T. Yasuhito, S. Shigeru, I. Yoshimasa, E. Patent 0,506,206 (1992).
[27] N. Frizi, P. Blanchard, E. Payen, P. Baranek, M. Rebeilleau, C. Dupuy, J.P. Dath, Catal. Today (2007), submitted.
[28] L. Benoist, D. Gonbeau, G. Pfister-Guillouzo, E. Schmidt, G. Meunier, A. Levasseur, Thin Solid Films 258 (1995) 110.
[29] S. Kasztelan, J. Grimblot, J.P. Bonnelle, E. Payen, H. Toulhoat, Y. Jacquin, Appl. Catal. 7 (1983) 91.
[30] C.B. Bloodworth, B. Demetriou, R. Grzeskowiak, Inorg. Chim. Acta 53 (1981) L85–L87.
[31] S.N. Rao, K.N. Munshi, N.N. Rao, M.M. Bhadbhade, E. Suresh, Polyhedron 18 (1999) 2491.
[32] D. Coucouvanis, A. Toupadakis, J.D. Lane, S.M. Koo, C.G. Kim, A. Haddjikyriacou, J. Am. Chem. Soc. 113 (1991) 5271.
[33] W.E. Newton, J.L. Corbin, J.W. McDonald, J. Chem. Soc. Dalton (1973) 1044.
[34] W.E. Newton, J.L. Corbin, D.C. Bravard, J.E. Searles, J.W. McDonald, Inorg. Chem. 13 (5) (1974) 1100.
[35] W. Yang, C. Lu, S. Lu, H. Zhuang, Helvet. Chim. Acta 85 (2002) 2417.
[36] I. Alstrup, I. Chorkendoff, R. Candia, B.S. Clausen, H. Topsøe, J. Catal. 77 (1982) 397.
[37] S. Eijsbouts, L.C.A. van den Oetelaar, R.R. van Puijenbroek, J. Catal. 229 (2005) 352.
[38] S. Texier, G. Berhault, G. Pérot, V. Harlé, F. Diehl, Catal. J. 223 (2004) 404.
[39] R. Candia, O. Sorensen, J. Villadsen, N.Y. Topsøe, B.S. Clausen, H. Topsøe, Bull. Soc. Chim. Belg. 93 (1984) 763.
[40] H. Schweiger, P. Raybaud, H. Toulhoat, J. Catal. 212 (2002) 33.
[41] S.L. Gonzalez-Cortés, T.-C. Xiao, P.M.F.J. Costa, B. Fontal, M.L.H. Green, Appl. Catal. A: Gen. 270 (2004) 209.
[42] E.J.M. Hensen, P.J. Kooyman, Y. van der Meer, A.M. van der Kraan, V.H.J. de Beer, J.A.R. van Veen, R.A. van Santen, J. Catal. 199 (2001) 224.